

The *HST* Large Programme on NGC 6752. I. Serendipitous discovery of a dwarf Galaxy in background*

L. R. Bedin^{1†}, M. Salaris², R. M. Rich³, H. Richer⁴, J. Anderson⁵, D. Bettoni¹,
D. Nardiello⁶, A. P. Milone⁶, A. F. Marino⁶, M. Libralato⁵, A. Bellini⁵, A. Dieball⁷,
P. Bergeron⁸, A. J. Burgasser⁹ and D. Apai^{10,11}

¹INAF-Osservatorio Astronomico di Padova, Vicolo dell'Osservatorio 5, I-35122 Padova, Italy

²Astrophysics Research Institute, Liverpool John Moores University, 146 Brownlow Hill, Liverpool L3 5RF, UK

³Department of Physics and Astronomy, UCLA, 430 Portola Plaza, Box 951547, Los Angeles, CA 90095-1547, USA

⁴Department of Physics and Astronomy, University of British Columbia, Vancouver, BC, V6T 1Z1, Canada

⁵Space Telescope Science Institute, 3800 San Martin Drive, Baltimore, MD 21218, USA

⁶Dipartimento di Fisica e Astronomia Galileo Galilei, Università di Padova, Vicolo dell'Osservatorio 3, Padova I-35122, Italy

⁷Argelander Institut für Astronomie, Helmholtz Institut für Strahlen-und Kernphysik, University of Bonn, Germany

⁸Département de Physique, Université de Montréal, C.P. 6128, Succ. Centre-Ville, Montréal, QC H3C 3J7, Canada

⁹Center for Astrophysics and Space Science, University of California San Diego, La Jolla, CA 92093, USA

¹⁰Department of Astronomy and Steward Observatory, The University of Arizona, 933 N. Cherry Avenue, Tucson, AZ 85721, USA

¹¹Lunar and Planetary Laboratory, The University of Arizona, 1640 E. University Blvd., Tucson, AZ 85721, USA

Accepted 201X XXXXXXXX XX. Received 201X XXXXXXXX XX; in original form 201X XXXXXX XX

ABSTRACT

As part of a large *Hubble Space Telescope* investigation aiming at reaching the faintest stars in the Galactic globular cluster NGC 6752, an ACS/WFC field was the subject of deep optical observations reaching magnitudes as faint as $V \sim 30$. In this field we report the discovery of *Bedin I*, a dwarf spheroidal galaxy too faint and too close to the core of NGC 6752 for detection in earlier surveys. As it is of broad interest to complete the census of galaxies in the local Universe, in this Letter we provide the position of this new object along with preliminary assessments of its main parameters. Assuming the same reddening as for NGC 6752, we estimate a distance modulus of $(m - M)_0 = 29.70 \pm 0.13$ from the observed red giant branch, i.e., $8.7^{+0.5}_{-0.7}$ Mpc, and size of $\sim 840 \times 340$ pc, about 1/5 the size of the LMC. A comparison of the observed colour-magnitude diagram with synthetic counterparts that account for the galaxy distance modulus, reddening and photometric errors, suggests the presence of an old (~ 13 Gyr) and metal poor ($[\text{Fe}/\text{H}] \sim -1.3$) population. This object is most likely a relatively isolated satellite dwarf spheroidal galaxy of the nearby great spiral NGC 6744, or potentially the most distant isolated dwarf spheroidal known with a secure distance.

Key words: dwarf galaxies: individual (Bedin I)

1 INTRODUCTION

New technologies and increasingly deep and wide surveys have resulted in the recent discovery of numerous dwarf spheroidal galaxies, principally in the vicinity of the Milky Way or M31. Only a handful of dwarf spheroidal galaxies with well established distances appear to be truly isolated. Cetus lies at 775 kpc from the Milky Way and 680 kpc from M31 (Whiting, Hau, & Irwin 1999; Lewis et al. 2007), Tu-

cana is roughly 900 kpc from the Milky Way and 1350 kpc from M31 (Lavery & Mighell 1992; Saviane et al. 1996), and KKR 25 at about 2 Mpc from both spirals is one of the most isolated (Makarov et al. 2012). The smallest of these stellar systems can exhibit either complex star formation histories, or more closely resemble the purely old, ~ 10 Gyr populations of the extended globular clusters in M31 (Huxor et al. 2005; Mackey et al. 2006). Although a number of possible additional cases are cited in Martinez-Delgado et al. (2018), the candidates usually lack secure distances, as the tip of the red giant branch (TRGB) becomes (under most circumstances) very difficult to measure at distances beyond 4 Mpc, even with *Hubble Space Telescope* (*HST*) imagery.

* Based on observations with the NASA/ESA *Hubble Space Telescope*, obtained at the Space Telescope Science Institute, which is operated by AURA, Inc., under NASA contract NAS 5-26555.

† E-mail: luigi.bedin@oapd.inaf.it

Any complex history of star formation makes the TRGB even harder to discern.

Here we report the discovery of one of the most distant, relatively isolated dwarf spheroidal galaxy with a secure TRGB distance. We have discovered this object serendipitously with extraordinarily deep *HST* images obtained for the purpose of investigating the white dwarf cooling sequence of the globular cluster NGC 6752.

2 OBSERVATIONS

All images for this study were collected with the *Wide Field Channel* (WFC) of the *Advanced Camera for Surveys* (ACS) at the focus of the *HST* under program GO-15096 (PI: Bedin). Unfortunately, five out of the planned 40 orbits failed because of poor guide star acquisition and will be reobserved at a later time. Usable data were collected between September 7 and 18, 2018, and consist of deep exposures of 1270 s each, 19 in the F814W filter, and 56 in F606W. Note that this is an astrometric multi-cycle programme, and a second epoch (also of 40 orbits) has already been approved (GO-15491) and scheduled for late 2019. Proper motions will eventually provide a near perfect field-object decontamination both for NGC 6752 members in the foreground, and for the members of the newly and serendipitously discovered stellar system in the background, to which we refer hereafter in this work as *Bedin I*. This object is worthy of early and separate publication as it is likely of general interest to the community as an example of a relatively isolated extragalactic system.

For completeness, Paper III of this series is focused on the white dwarfs of NGC 6752 in this very same ACS/WFC field, while Paper II deals with multiple stellar populations detected within NGC 6752 in our parallel observations with the *Infra-Red channel* (IR) of the *Wide Field Camera 3* (WFC3).

3 DATA REDUCTION AND ANALYSIS

All images were pre-processed with the pixel-based correction for imperfections in the charge transfer efficiency (CTE) with the method described in Anderson & Bedin (2010). Photometry and relative positions were obtained with the software tools described by Anderson et al. (2008). In addition to solving for positions and fluxes, important diagnostic parameters were also computed, such as the image-shape parameter, which quantifies the fraction of light that a source has outside the predicted point-spread function (PSF). This is useful for eliminating the faint unresolved galaxies that tend to plague studies of faint point sources.

The astrometry was registered to International Celestial Reference System (ICRS) using sources in common with Gaia DR2 (Gaia collaboration 2018) with tabulated proper motions transformed to the epoch 2018.689826 of *HST* data, following the procedures in Bedin & Fontanive (2018).

The photometry was calibrated on the ACS/WFC Vega-mag system following the procedures given in Bedin et al. (2005) using encircled energy and zero points avail-

able at STScI.¹ For these calibrated magnitudes we will use the symbols m_{F606W} and m_{F814W} .

The software also corrects for distortion in all the images and transforms their coordinates to a common reference frame after removal of cosmic rays and most of the artifacts. It then combines them to produce stacked images that, at any location, give sigma-clipped values of the individual values from pixels of all images at that location.

In Fig. 1 we show a portion of a pseudo-trichromatic stack containing Bedin I. [Note that we adopted the F814W images for the red channel, the F606W ones for the blue channel, and computed a wavelength weighted (blue/red \sim 3) average of the two for the green channel.] In these images the dwarf spheroidal clearly appears. Unfortunately the system is close to the border of the field, where the depth of the coverage is lowered by the large dithers strategy employed for this programme, and its view is incomplete (particularly in F814W).

We attempted to fit an ellipse to derive the luminosity profile (Jedrzejewski et al. 1987), however there are several much brighter foreground stars superimposed on the faint galaxy. To be able to fit the underlying galaxy, we masked all contaminating sources by hand as well as all the visible diffraction spikes. We used the images in the F606W filter, as they cover a larger area and reach deeper magnitude than those in F814W. A single Sersic function (Sersic 1963, see also Graham et al. 2005) was used as model, allowing all parameters to vary. The final fit gives parameters for Bedin I listed in Table 1. However, these values should be treated as indicative, given the level of contamination and the incomplete view of the system. Figure 1 show the fitted ellipse at an extension where the profile drops to zero (in green), and at the half-luminosity radius (in magenta).

Given the uncertainties of this fit, and the physical linear edge of the fov, we define the dwarf-galaxy sample within boxes rather than ellipses. In the left panel of Fig. 2 we show the colour-magnitude diagram (CMD) for all measured stars within a box of $75'' \times 110''$ containing Bedin I (grey points), and the closest one to the centre of the system, within a $15'' \times 30''$ box (black points). This CMD shows clearly a red giant branch (RGB) that appears to end around $m_{F814W} = 25.6\text{--}25.8$. We then defined by-eye a fiducial line (shown in red) representative of the RGB, extending beyond the apparent TRGB.

Next, we performed artificial-star tests (ASTs) within the same box containing Bedin I; these ASTs were performed using the procedures described by Anderson et al. (2008). Artificial stars were added in a magnitude range $m_{F814W} = 20\text{--}29$ with a flat distribution, with colours that placed them on the fiducial RGB, to determine completeness and to estimate errors; the resulting CMD for ASTs is shown in the right panel of Fig. 2 along with the derived completeness (green line). [Note the rather low completeness $\sim 45\%$ at the TRGB level, because a large fraction of the area is disturbed by the halos of saturated stars, see Fig. 1.]

¹ <http://www.stsci.edu/hst/acs/analysis/zeropoints>

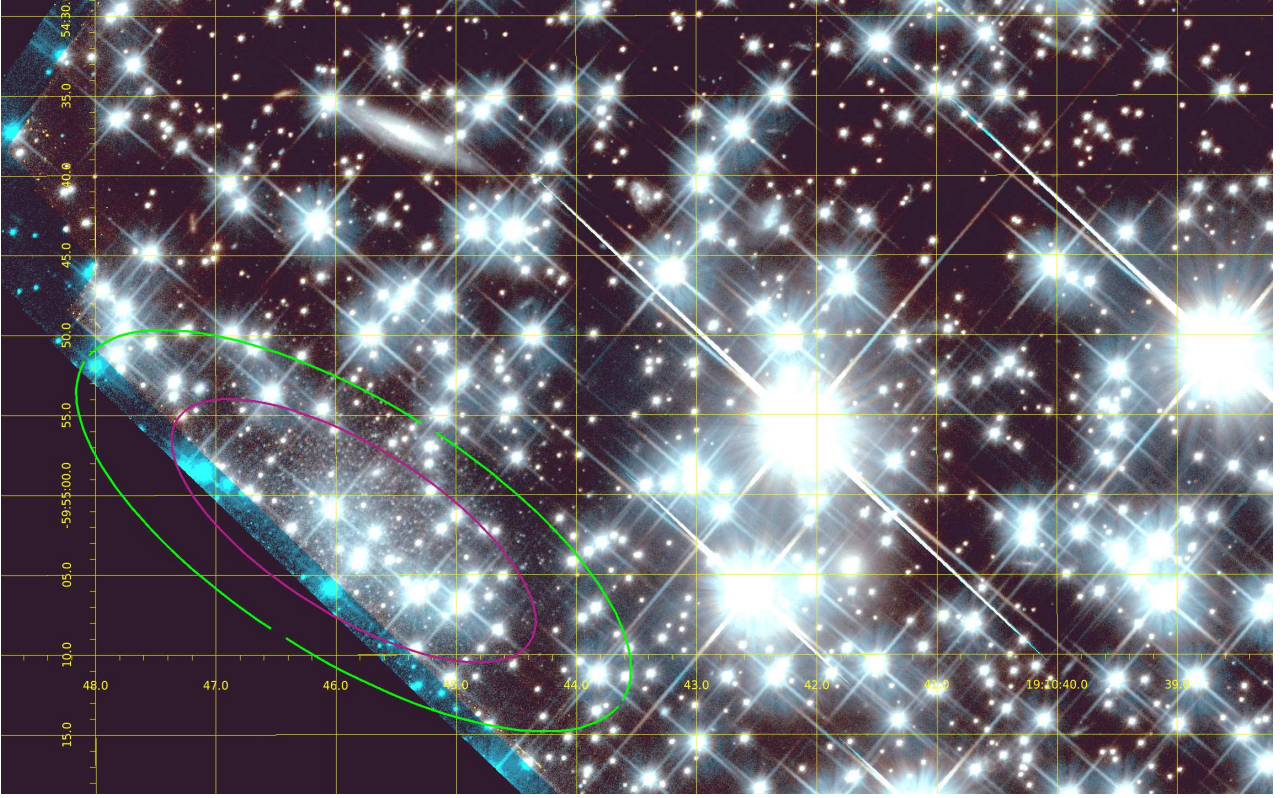


Figure 1. A $80'' \times 50''$ portion of the ACS/WFC field containing Bedin I. North is up, East to the left (ICRS coordinates grid in yellow). Unfortunately, Bedin I is very close to the border of the field of view (fov), where the large dithers gave us an overall incomplete (particularly in the red filter) and shallower view with respect to the centre of the fov. This portion of the field contains what is available to us of the new dwarf spheroidal, and extends West to show an adjacent region for comparison. The green ellipse marks the limit to where Bedin I seems to extend, while the one in magenta denotes the fitted half-light radius (see text).

Table 1. Properties of *Bedin I* dwarf spheroidal galaxy.

α_{ICRS}	$19^{\text{h}}:10^{\text{m}}:45^{\text{s}}.85$
δ_{ICRS}	$-59^{\circ}:55':02''.25$
ℓ	$336^{\circ}56365$
b	$-25^{\circ}60333$
r_e (effective half-light radius)	$\sim 8.3''$ (~ 350 pc)
$\epsilon = \frac{a-b}{a}$	0.6
$a_{\text{max-axis}}$	$\sim 20''$ (~ 840 pc)
$b_{\text{max-axis}}$	$\sim 8''$ (~ 340 pc)
P.A.	58°
$E(m_{\text{F606W}} - m_{\text{F814W}})$	0.04
$(m - M)_0$	29.70 ± 0.13
d	$8.7^{+0.5}_{-0.7}$ Mpc
m_{F606W}	19.94
M_{F606W}	-9.76
μ_{F606W}	$26.78 \text{ mag/arcsec}^2$

4 DISTANCE AND METALLICITY

Based on the data displayed in Fig. 2 we have made a rough formal estimate of distance and metallicity of this galaxy. For the distance we employed the TRGB absolute magnitude-colour relation in the ACS/WFC system by Rizzi

et al. (2007):

$$M_{\text{F814W}}^{\text{TRGB}} = -4.06 + 0.20[(m_{\text{F606W}} - m_{\text{F814W}})_{\text{TRGB}} - 1.23] \quad (1)$$

An edge detection algorithm with kernel $[-1 \ 0 \ +1]$ (Sobel filter, see, e.g., Madore & Freedman 1995) was employed to determine the TRGB m_{F814W} apparent magnitude, considering all stars within the $75'' \times 110''$ box containing Bedin I (black and grey points in Fig. 2). There are about 50 stars (without accounting for the effect of completeness) in the upper magnitude bin below $m_{\text{F814W}}=25.5$, that seems to be approximately the location of the TRGB. With this sample size, systematic errors on the location of the TRGB using a Sobel filter are below 0.1 mag (Madore & Freedman 1995).

We have determined the m_{F814W} differential luminosity function (LF) for the RGB stars with m_{F814W} between ~ 23 and 28 mag, in 0.25 mag bins (this width corresponds to 2-3 times the 1σ photometric error estimated from the ASTs for $m_{\text{F814W}} < 27.0$), and applied our derived completeness corrections to star counts in each bin.

We then applied the Sobel's edge-detection algorithm to this completeness corrected LF; a sharp spike in the filter output (see middle panel of Fig. 3) marks the position of TRGB, that we take as the midpoint of the bin corresponding to the spike. We have repeated several times this procedure by changing the magnitude of the initial point of the brightest bin by 0.01 mag at a time, and determined $m_{\text{F814W}}^{\text{TRGB}} = 25.70 \pm 0.13$.

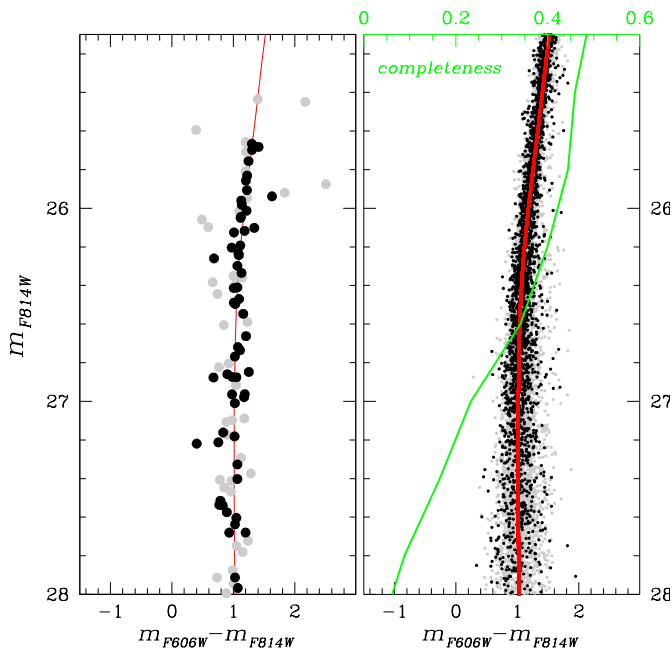


Figure 2. (*Left panel:*) CMD of all stars in the region of Bedin I (grey) and for just those ones closest to its centre (in black, see text). The fiducial line defined by-eye and used to generate artificial stars, is displayed in red. (*Right panel:*) Same CMD but for the artificial stars in the same regions (using same colour code) added along the fiducial line (in red). We also show the derived completeness function (in green), whose values can be read on the top axis.

As for the TRGB colour to employ in Eq. 1, an histogram of the colour distribution (0.1 mag bins) for all stars with m_{F814W} between 25.53 and 25.83 mag discloses a clear peak at $(m_{F606W} - m_{F814W})_{\text{TRGB}} = 1.22 \pm 0.05$ that we take as the galaxy TRGB mean colour.

We assumed a reddening $E(B - V) = 0.04$ as for NGC 6752 (Harris 1996, updated by December 2010), corresponding to $A_{F606W} = 0.11$, $A_{F814W} = 0.07$, following the extinction law in the ACS/WFC photometric system determined by Bedin et al. (2005). This gives a dereddened TRGB colour $(m_{F606W} - m_{F814W})_{\text{TRGB}} = 1.18 \pm 0.05$. By using the TRGB absolute magnitude calibration of Eq. 1 we obtained a distance modulus $(m - M)_0 = 29.70 \pm 0.13$, corresponding to a linear distance of about $8.7^{+0.5}_{-0.7}$ Mpc.

Figure 3 also displays a qualitative comparison of the galaxy CMD with a synthetic counterpart², obtained employing scaled-solar BaSTI isochrones (Pietrinferni et al. 2004) for an age of 13 Gyr and $[\text{Fe}/\text{H}] = -1.27$. We have included photometric errors in both m_{F814W} and m_{F606W} as derived from the ASTs, and shifted the CMD of the synthetic population by $(m - M)_0 = 29.70$, $A_{F606W} = 0.11$ and $A_{F814W} = 0.07$. The synthetic CMD nicely overlaps with the observational counterpart. Its colour width is quite comparable with the observed one, and the theoretical TRGB agrees with the edge detection results. This suggests that, within

² The number of synthetic stars below the model TRGB is the same as the number of observed stars below the TRGB as identified by the edge detection algorithm.

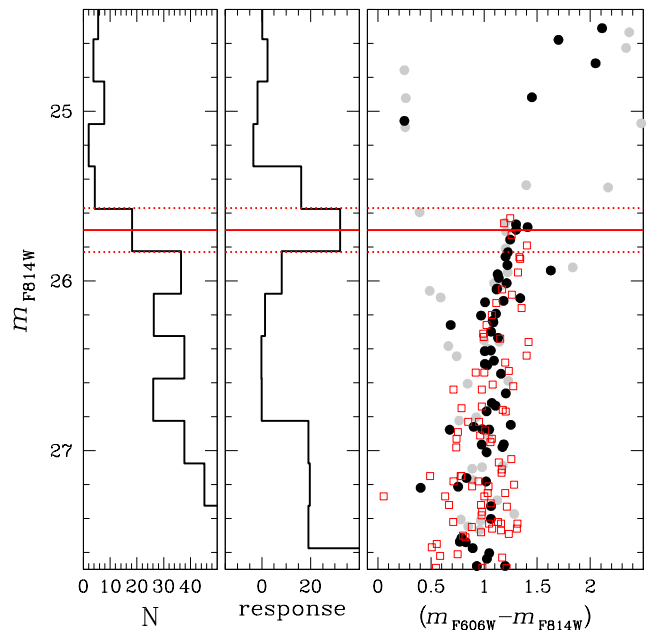


Figure 3. The left and middle panel display, respectively, the observed LF of the galaxy upper RGB, and the output of the edge detection algorithm. The position of the TRGB is marked with a red solid line, while the dotted lines give the uncertainty (see text for details). The right panel displays the galaxy RGB (symbols as in Fig. 2) and a synthetic CMD (red squares) for a 13 Gyr old, $[\text{Fe}/\text{H}] = -1.27$ population (see text for details).

the current photometric errors, the observed galaxy population is quite homogeneous, similar to typical metal poor globular clusters.

Notably, the CMD resembles that of a number of M31 dwarf spheroidal galaxies (Martin et al. 2017). It is unlikely that any new observations might reach the red clump/horizontal branch, that could contain interesting information on the system’s age.

5 CONCLUSIONS

We conclude that this object is most likely an isolated dwarf spheroidal galaxy, but could be associated with NGC 6744. Indeed, NGC 6744 has a distance of 9.15 ± 0.40 Mpc (Tully et al. 2013 catalog gives $(m - M)_0 = 29.81 \pm 0.09$), i.e., consistent with the dwarf within uncertainties, and it is at an angular distance of about 4 degrees from the dwarf spheroidal (so, at a minimum distance of ~ 650 kpc on the plane of the sky). The galaxy NGC 6744 is a Milky-Way-analog barred spiral with $M_V = -21.8^3$, a member of the Pavo group, and has a low luminosity AGN (da Silva et al. 2018).

The size and the estimated ellipticity of Bedin I offer the closest resemblance to the Tucana dwarf spheroidal galaxy (see e.g., Fraternali et al. 2009). KKR 25 is an almost identical isolated dwarf system, with similar luminosity ($M_V \sim -10.93$), ellipticity, and color-magnitude diagram (Makarov et al. 2012). The new system is both too

³ ned.ipac.caltech.edu

large, and insufficiently compact, to be classified alongside the extended globular clusters of M31 (Huxor et al. 2005). At $M_{F606W} \sim -10$, the system would be among the more luminous M31 dwarf spheroidal galaxies. The half-light effective radius ($r_e \sim 350$ pc) and ellipticity place it comfortably among the M31 dwarfs spheroidals (Martin et al. 2017) and the Milky Way dwarfs (Collins et al. 2014). The system also appears to have had a quiet star formation history, with a red giant branch resembling that of the majority of M31 dwarf spheroidal galaxies (Martin et al. 2017). The narrow RGB and $[\text{Fe}/\text{H}] = -1.3$ admits little internal production of metals, and our limited sample of sufficiently well-measured stars show no obvious or sizable population of AGB or younger stars. Our photometry is too shallow to reach the horizontal branch, that would provide additional constraints on both the distance and star formation history, and such faint magnitudes may be beyond any current or contemplated facilities. Considering the isolation of the system relative to any luminous galaxy, it is curious that the RGB is extremely narrow, implying little internal production of metals, suggesting a chemical evolution closer to that of globular cluster than a fully fledged dwarf galaxy. We conclude that this system likely formed more than 10 Gyr ago in a “single” burst, and likely experienced no additional star formation since its formation. The reasonably well-determined distance of this system makes it one of the best candidates for a relatively isolated dwarf spheroidal galaxy.

As a final remark, it is interesting to compare Bedin I with the faint dwarf irregular galaxy *LV J1157+5638 sat* discovered by Makarova et al. (2018). A comparison to Fig. 5 of Makarova et al. (2018) shows that Bedin I is very likely among the least luminous galaxies known at a distance of more than 4 Mpc. Both systems were discovered serendipitously in deep *HST* imaging. These two works bode well for the potential of the High Latitude Survey planned for the Wide Field Infrared Survey Telescope (*WFIRST*)⁴ to reveal a statistical population of similar objects.

ACKNOWLEDGMENTS

We are grateful to an anonymous referee for his/her prompt review of our work. This work is based on observations with the NASA/ESA Hubble Space Telescope, obtained at the Space Telescope Science Institute, which is operated by AURA, Inc., under NASA contract NAS 5-26555. J.A., R.M.R., A.B., M.L., and acknowledge support from *HST*-GO-15096. A.P.M. acknowledge funding from the European Research Council (ERC) under the European Union’s Horizon 2020 research innovation programme (Grant Agreement ERC-StG 2016, No 716082 ‘GALFOR’. APM acknowledges support from MIUR through the the FARE project R164RM93XW SEMPLICE. AFM has received funding from the European Unions Horizon 2020 research and innovation programme under the Marie Skłodowska-Curie Grant Agreement No. [797100].

REFERENCES

- Anderson, J., Sarajedini, A., Bedin, L. R., King, I. R., Piotto, G., Reid, I. N., Siegel, M., Majewski, S. R., Paust, N. E. Q., Aparicio, A., Milone, A. P., Chaboyer, B., & Rosenberg, A. 2008, *AJ*, 135, 2055
- Anderson, J., & Bedin, L. R. 2010, *PASP*, 122, 1035
- Bedin, L. R., Cassisi, S., Castelli, F., Piotto, G., Anderson, J., Salaris, M., Momany, Y., & Pietrinferni, A. 2005, *MNRAS*, 357, 1038
- Bedin, L. R., & Fontanive, C. 2018, *MNRAS*, 481, 5339
- Collins, M. L. M. et al. 2014, *ApJ*, 783, 7
- da Silva, P., Steiner, J. E. and Menezes, R. B. 2018, *ApJ*, 861, 83
- Fraternali, F. et al. 2009, *A&A*, 499, 121
- Gaia Collaboration, Brown, A. G. A., Vallenari, A., et al. 2018, *A&A*, 616, A1
- Graham, A. W., & Driver, S. P. 2005, *PASA*, 22, 118
- Jedrzejewski, R. I., Davies, R. L., & Illingworth, G. D. 1987, *AJ*, 94, 1508
- Harris, W. E. 1996, *AJ*, 112, 1487
- Huxor, A. P., Tanvir, N. R., Irwin, M. J., Ibata, R., Collett, J. L., Ferguson, A. M. N., Bridges, T., & Lewis, G. F. 2005, *MNRAS*, 360, 1007
- Lavery, R. J., & Mighell, K. J. 1992, *AJ*, 103, 81
- Lewis, G. F., Ibata, R. A., Chapman, S. C., McConnachie, A., Irwin, M. J., Tolstoy, E., & Tanvir, N. R. 2007, *MNRAS*, 375, 1364
- Mackey, A. D., Huxor, A., Ferguson, A. M. N., Tanvir, N. R., Irwin, M., Ibata, R., Bridges, T., Johnson, R. A., & Lewis, G. 2006, *ApJL*, 653, L105
- Madore, B. F., & Freedman, W. L. 1995, *AJ*, 109, 1645
- Makarov, D. et al. 2012, *MNRAS*, 425, 709
- Makarova, L. N., Makarov, D. I., Antipova, A. V., Karachentsev, I. D., & Tully, R. B. 2018, *MNRAS*, 474, 3221
- Martin, N. F., Weisz, D. R., Albers, S. M., Bernard, E., Collins, M. L. M., Dolphin, A. E., Ferguson, A. M. N., Ibata, R. A., Laevens, B., Lewis, G. F., Mackey, A. D., McConnachie, A., Rich, R. M., & Skillman, E. D. 2017, *ApJ*, 850, 16
- Martinez-Delgado, D., Grebel, E. K., Javanmardi, B., Boschin, W., Longeard, N., Carballo-Bello, J. A., Makarov, D., Beasley, M. A., Donatiello, G., Haynes, M. P., Forbes, D. A., & Romanowsky, A. J. 2018, arXiv:1810.04741
- Pietrinferni, A., Cassisi, S., Salaris, M., & Castelli, F. 2004, *ApJ*, 612, 168
- Rizzi, L., Tully, R. B., Makarov, D., Makarova, L., Dolphin, A. E., Sakai, S., & Shaya, E. J. 2007, *ApJ*, 661, 815
- Saviane, I., Held, E. V., & Piotto, G. 1996, *A&A*, 315, 40
- Sérsic, J. L. 1963, *Boletín de la Asociación Argentina de Astronomía La Plata Argentina*, 6, 41
- Tully, R. B. et al. 2013, *AJ*, 146, 86
- Whiting, A. B., Hau, G. K. T., & Irwin, M. 1999, *AJ*, 118, 2767

⁴ <https://wfirst.gsfc.nasa.gov/>,
<https://www.wfirst-hls-cosmology.org/>